

UHECR source statistics in the GZK energy range

C. BLAKSLEY¹, E. PARIZOT¹, D. ALLARD¹

¹ *Laboratoire Astroparticule et Cosmologie (APC), Université Paris 7 / CNRS, 10 rue A. Domon et L. Duquet, 75205 Paris Cedex 13, France*

Abstract: The GZK effect, i.e. the interaction of ultra-high-energy cosmic ray (UHECR) protons and nuclei with the intergalactic photon background, results in a drastic reduction of the number of sources contributing to the observed flux above ~ 60 EeV. We study quantitatively the source statistics as a function of energy for a range of models compatible with the current data, varying the source composition and injection spectrum, as well as the source density and luminosity distribution, and exploring various realizations of the source distribution. We find that, in typical cases, the brightest source in the sky contributes more than 20% of the total flux above 80 EeV, and about 1/3 of the total flux at 100 EeV. We also show that typically between 2 and 5 sources contribute more than half of the UHECR flux at 100 EeV. With such low source numbers, the isolation of the few brightest sources in the sky may be possible for experiments collecting sufficient statistics at the highest energies, even in the event of relatively large particle deflections. In addition, we study the effect of detector energy resolution on these results.

Keywords: cosmic rays, ultra-high-energy, GZK, UHECR models, source density, astroparticle

1 Introduction

The last decade has established ultra-high-energy cosmic ray (UHECR) physics as a phenomenologically rich and experimentally mature science. Key observations related to the UHECR energy spectrum [13, 7, 21], composition [14, 5, 8, 20], and distribution over the sky [6, 15, 22] have clarified some open questions, notably the existence of a strong decrease in the UHECR flux above ~ 60 EeV. These same observations have also raised new questions. The question of composition has become central due to both new observational results and a greater understanding of the interplay between composition and general UHECR phenomenology. This includes constraints on individual source spectra and power, maximum energy, and source evolution [9, 2, 4, 1, and refs. therein].

The absence of a clear signal of anisotropy or correlation with some classes of astrophysical objects has raised doubts about the utility of pursuing the quest for the highest energy particles in the universe. Even if large deflections at ultra-high-energy due to large particle charges or strong magnetic fields are a reality, however, individual sources could still be isolated in the sky if the UHECR flux is dominated by the contribution of a limited number of sources.

As the energy of cosmic-ray particles increases, their propagation length decreases due to their interaction with the photon background, and the contribution of far-away sources is attenuated with increasing energy in what is known as the GZK effect [12, 24]. The reduction of the horizon associated with the GZK effect implies that fewer and fewer sources contribute to the flux at higher and higher energy. In this regard, the GZK effect can turn into a useful phenomenon, provided that the low statistics implied can be overcome in future experiments.

We address this question quantitatively by studying the contribution of individual sources to the overall flux, focusing on the number of contributing sources as a function of energy. We simulate several astrophysical scenarios with different source densities, source spectra, and compositions. We also study the “cosmic variance” associated with differ-

ent possible realizations and explore the effect of a distribution of intrinsic source luminosity. The study of particle deflections, and the drawing of realistic sky-maps, are left to another work (see [19], this conference).

2 The method

The fraction of the flux actually contributed by each source at a given energy depends on its actual distance, intrinsic power, and precise attenuation due to the intervening interactions. To study the combination of these effects, we do Monte-Carlo simulations using a previously developed and well-tested propagation code [3, 1]. This code can be applied to models with various source spectra, compositions, powers, spatial distributions, and cosmological evolutions.

We explore numerous combinations, with the requirement that the resulting propagated energy spectrum is compatible with current data. We chose four that include both conservative and extreme cases: a pure proton model, a pure Fe model, a generic mixed composition model, and the so-called low proton E_{\max} model [2, 3], which accounts for a possible evolution towards a heavier composition above 10 EeV [8]. The spectrum is assumed to be a power law of index x , with an exponential cutoff above energy E_{\max} for protons, and $Z \times E_{\max}$ for nuclei of charge Z [1, 11].

The parameters used correspond to those that best fit the Auger data, but no significant impact on these results was found when using values obtained by fitting the HiRes data instead. The values of E_{\max} in each scenario are adjusted, together with the source spectral index and composition enhancement, to reproduce the observed cutoff in the UHECR spectrum without introducing unobserved features around the maximum proton energy¹.

In all cases, we assume that there is no evolution of the intrinsic source power or density as a function of red-shift. To investigate the influence of such evolution,

1. For complete details of the parameters see the published version of this article [10]

we considered a mixed composition model with strong cosmological evolution using an SFR [16] or an FRII [23] evolution model. For either model the effect on our results was negligible.

We assume, by default, that the sources each have the same power, but we also study the effect of a distribution of intrinsic source luminosity. We do this by considering the same models, but assigning each source a luminosity according to either a \log_{10} -normal distribution with a σ of either 1 or 2 or a power law distribution with an index of -2.

For each model, we build three different scenarios, corresponding to three choices of source density: $n_s = 10^{-4}$, 10^{-5} , and 10^{-6} Mpc^{-3} . The highest density is representative of the AGN density in the local universe. The lowest density corresponds to an average of ~ 4 sources within 100 Mpc.

For each of these scenarios, we build a particular realization of the source configuration with the assumed density by drawing a subsample of galaxies in the flux-limited 2MRS catalog [17] up to a limiting radius, R_{limit} , beyond which we assume a continuous source distribution. In the case of a distribution of intrinsic source luminosities, each source is assigned a random luminosity according to the chosen distribution.

We then propagate hundreds of thousands of UHECRs emitted by each of the sources according to their assumed spectrum and composition. The UHECR reaching Earth are collected into a sufficiently large data set to avoid statistical fluctuations, and from this data set we determine the fraction of events which come from each source. This fraction depends on the energy of the UHECRs, and we study the evolution of this fraction as a function of energy by considering only UHECR events above a given minimum energy, E_{min} . As the actual universe is a definite, but a priori unknown realization of the underlying astrophysical scenario, we must explore the cosmic variance associated with different source configurations. We therefore repeat the above procedure for 50 different source configurations with the same density within the same astrophysical model and analyze the distribution of results.

3 Results

To address the number of sources visible in the sky and their respective weight we determine for each of the scenarios described in section 2 the fraction of UHECRs contributed by all sources and sort the sources by this apparent luminosity. We present the value of the median of the distributions as the typical value to be expected for a given scenario, along with a 68% probability interval around the median value.

In Fig. 1, we show the evolution of the fractional contribution of the three brightest sources as a function of minimum energy, E_{min} , for the mixed composition model with a source density of $n_s = 10^{-5} \text{ Mpc}^{-3}$. The contribution of the brightest sources increases with the energy, which is a direct consequence of the GZK effect. The fractional contribution of the second brightest source is typically a factor of 2–2.5 lower than that of the brightest source, and the contribution of the third brightest source is another factor of two lower. This hierarchy is clear when looking at the median of the distributions, but two or three sources may contribute roughly equally to the UHECR flux in individual realizations, as suggested by the 68% spread in the plot.

In Fig. 2 we compare the fractional contribution of the brightest source between models and source densities by plotting the median for each scenario as a function

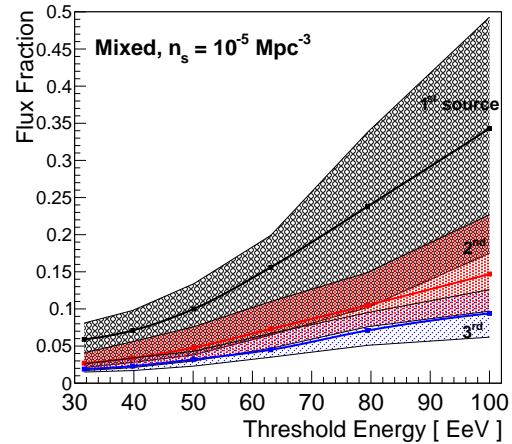


Figure 1: Median flux as a percentage of the total for the brightest 3 sources in the sky shown for a mixed-composition model with a source density of $n_s = 10^{-5}$

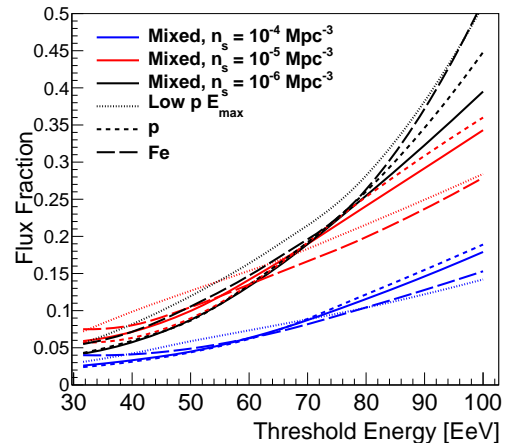


Figure 2: Median flux as a percentage of the total for the brightest source in the sky, shown for all four models and for source densities of $n_s = 10^{-4}$, 10^{-5} , and 10^{-6} Mpc^{-3} .

of E_{min} . At a given density, the difference between the contributions of the brightest source in the four models is relatively moderate, of the order of a 20% relative variation at $E_{\text{min}} = 100 \text{ EeV}$. However, a large difference can be seen for each model between the three source densities. At $E_{\text{min}} = 100 \text{ EeV}$, the typical fractional contribution is a factor of two larger at $n_s = 10^{-5} \text{ Mpc}^{-3}$ than at $n_s = 10^{-4} \text{ Mpc}^{-3}$, and another 50% more at $n_s = 10^{-6} \text{ Mpc}^{-3}$.

The domination of a few sources in the UHECR flux increases as the source density decreases, due primarily to the fewer number of sources overall. But as can also be seen, this effect is reduced at low energy. This is because the contribution of the most nearby sources, for which the actual density makes a difference (compared to a continuous distribution of sources), is reduced as the GZK horizon recedes. At the lowest energies considered here, $\sim 30 \text{ EeV}$, the horizon scale is much larger than the distance between neighboring sources and R_{limit} . As a consequence, the

increase of the fractional contribution of the brightest source with energy is stronger for lower densities.

To investigate the influence of different luminosity distributions, as discussed in Sect. 2, we considered the evolution with energy of the median fractional contribution of the brightest source for a mixed composition model with $n_s = 10^{-5} \text{ Mpc}^{-3}$. The contribution increases in every case, passing from 34% at 100 EeV in the case of standard candles to up to 47% for the \log_{10} -normal, $\sigma = 1$, scenario. This is because upward fluctuations, where one nearby source is brighter than average, extend the distribution towards higher fractional contributions, while downward fluctuations simply switch the ordering of the source brightnesses.

It is also interesting to determine how many sources are expected to make up more than, say, 50% of the flux in each scenario. This number, denoted by $N_{50\%}$, is shown in Fig. 3 for the mixed composition model and three values of the source density, and in Fig. 4 for each of the four models with a density $n_s = 10^{-5} \text{ Mpc}^{-3}$.

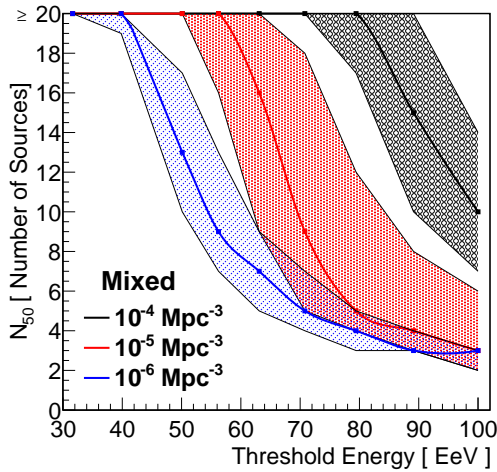


Figure 3: The number of sources (starting from the highest percentage contributor) which provide at least 50% of the total flux, $N_{50\%}$, as a function E_{\min} , the minimum event energy. $N_{50\%}$ is shown for a mixed-composition model with source densities of $n_s = 10^{-4}, 10^{-5}$, and 10^{-6} Mpc^{-3} . The shaded contours show the region which contains 68% of all realizations.

The strongest influencing parameter is again source density. For $n_s = 10^{-5} \text{ Mpc}^{-3}$, $N_{50\%}$ is between three and four at $E = 100 \text{ EeV}$. At 80 EeV, $N_{50\%}$ moderately increases to between four and seven. However, below 80 EeV, it rapidly increases as a result of the quickly receding horizon to reach more than 20 sources needed to make up more than 50% of the flux. This is a direct demonstration of the GZK effect, and the dramatic decrease in the overall UHECR spectrum above 60 EeV is due to the reduction in the number of contributing sources in that energy range.

The source density influences $N_{50\%}$ as expected: fewer sources contribute a large fraction of the flux at lower densities, and a handful of sources make up 50% of the flux down to 60 EeV for $n_s = 10^{-6} \text{ Mpc}^{-3}$, instead of 80 EeV for $n_s = 10^{-5} \text{ Mpc}^{-3}$. For source densities as high as $n_s = 10^{-4} \text{ Mpc}^{-3}$, $N_{50\%}$ is greater than ten even at 100 EeV. For a given model, a distribution of source luminosities results in a lower value of $N_{50\%}$ compared to the same

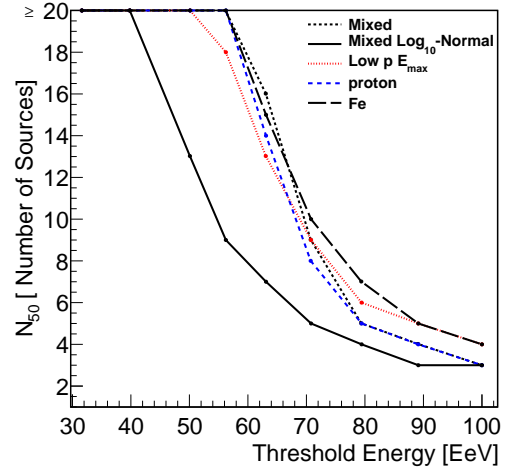


Figure 4: $N_{50\%}$ for a source density of $n_s = 10^{-5} \text{ Mpc}^{-3}$ for each model, and, in addition, a mixed-composition model with source luminosities distributed according to a \log_{10} -normal distribution with $\sigma = 1$. Here, the 68% contours are omitted for clarity. (See Fig.3 for details)

scenario assuming standard candle sources, as can be seen in Fig. 4.

A further question is the effect of an imperfect energy resolution on these results. Experimentally, a cut in the UHECR energy, as assumed above, cannot be perfectly applied as some lower energy events will be (mis-)reconstructed at higher energy. These events will contaminate the energy range where very few sources contribute to the overall flux with UHECRs from additional sources within the lower energy horizon. As the UHECR spectrum rapidly decreases as energy increases, a small fraction of events reconstructed with an upward fluctuation of the estimated energy can represent a significant fraction of the events attributed to a higher energy bin.

To illustrate this effect, we implemented a Gaussian detector response when binning each UHECR event with respect to E_{\min} and performed the analysis with the reconstructed energies. The results are shown in Fig. 5 for a detector with 10%, 20%, and 30% energy resolution, overlaid with the results for a perfect detector. As expected, a deterioration of the energy resolution results in a smaller contribution of the brightest source to the UHECR events above any given energy. For our fiducial mixed-composition model with source density $n_s = 10^{-5} \text{ Mpc}^{-3}$, this fraction goes from 24% for perfect resolution at 80 EeV to respectively 23%, 19%, and 17%.

The ability of a given detector to actually isolate the brightest sources in the sky thus depends on its energy resolution. The energy dependence of the detector acceptance will also play a role if, for example, lower energy events have a lower probability of being detected. This should thus be modeled for each experiment, given its individual characteristics.

4 Conclusion

Above $E > 3 \cdot 10^{19} \text{ eV}$ the number of sources that contribute to the UHECR flux can be expected to strongly decrease, down to only a few sources at the highest energies. This

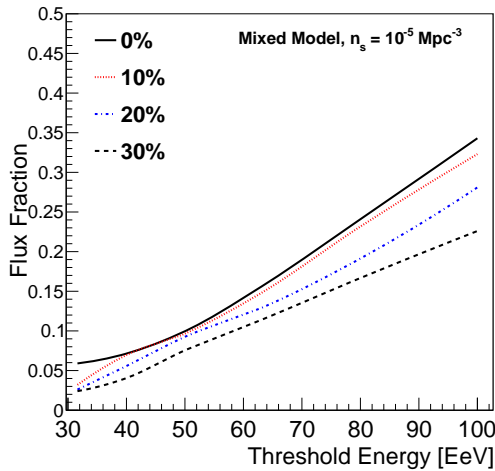


Figure 5: Median flux fraction of the brightest source in the sky as a function of minimum *reconstructed* energy, shown for a mixed-composition model with a source density of $n_s = 10^{-5} \text{ Mpc}^{-3}$. The top curve shows a perfect energy reconstruction, and the lower three correspond to detectors with a Gaussian energy resolution of 10%, 20%, and 30%.

decrease is due to the energy loss length of protons and heavy nuclei during propagation from their sources to the Earth, i.e. the GZK effect. To quantify this effect, we have shown results for the fractional contribution of the brightest sources in the UHECR sky as a function of minimum threshold energy. Because the exact contribution is dependent on the spatial configuration of the closest sources, we reported the median value over a set of realizations and for three choices of source density. We considered several UHECR source scenarios with respect to composition and energy spectrum. The choice of source parameters was motivated by previous studies of UHECR propagation so as to fit the data.

For a mixed-composition model with a source density of $n_s = 10^{-5} \text{ Mpc}^{-3}$, we find that above $E = 100 \text{ EeV}$ the brightest UHECR source in the sky can be expected to contribute, as a median, $34^{+15}_{-17}\%$ of the total flux, and the brightest three sources contribute more than 50% of the total flux. For lower source densities, the UHECR sky at the highest energies is dominated by even fewer sources. Scenarios with $n_s = 10^{-6} \text{ Mpc}^{-3}$ typically result in three or four sources making up more than 50% of the flux down to 80 EeV, and can leave only one or two sources contributing half of the total flux above 100 EeV.

The results presented in this paper assume that the UHECR sources are standard candles, although it is likely that they distribute over a range of intrinsic luminosities. This will increase, on average, the weight of the most luminous sources in the overall UHECR sky. We quantified this effect for a representative choice of source luminosity distributions, and found that the contribution of the brightest source increases to $43^{+26}_{-16}\%$ for a log-normal distribution with $\sigma = 1$ and a source density $n_s = 10^{-5} \text{ Mpc}^{-3}$, at 100 EeV. In such a scenario, two sources largely dominate the observed flux at this energy.

The results presented here illustrate the importance of concentrating on the highest energies, right inside the GZK cutoff, in order to take full advantage of the GZK effect and

the associated reduction of the number of visible sources. In particular, Figs. 3 and 4 shows that a dramatic change in this number occurs between 50 EeV and 80 EeV. This suggests that a significant increase in the clustering signal can be expected if a new generation of detectors can be used to push the current statistics achieved at 50 or 60 EeV up to 80 or 100 EeV.

References

- [1] Allard, D., 2011, arXiv:1111.3290
- [2] Allard, D., Parizot, E., & Olinto, A. V., 2007, *Astroparticle Physics*, 27, 61
- [3] Allard, D., Busca, N. G., Decerprit, G., Olinto, A. V., & Parizot, E., 2008, *JCAP*, 10, 33
- [4] Aloisio, R., Berezhinsky, V., Blasi, P., Gazizov, A., Grigorieva, S., & Hnatyk, B., 2007, *Astroparticle Physics*, 27, 76
- [5] The Pierre Auger Collaboration, *Phys. Rev. Lett.*, 2010, 104, 091101
- [6] The Pierre Auger Collaboration, 2010, *Astropart. Phys.*, 34, 314
- [7] The Pierre Auger Collaboration, 2011, *Nuclear Instruments and Methods in Physics Research A*, 630, 91
- [8] The Pierre Auger Collaboration, *Proc. of the 32nd ICRC, Beijing, China, 2011*, arXiv:1107.4804v1
- [9] Berezhinskii, V. S., & Grigor'eva, S. I., 1988, *A&A*, 199, 1
- [10] Blaksley, C., Parizot, E., Decerprit, G., & Allard, D., 2013, *Astronomy and Astrophysics*, 552, A125
- [11] Duvernois, M. A. & Thayer, M. R., 1996, *ApJ*, 465, 982
- [12] Greisen K. 1966, *Phys. Rev. Lett.* 16, 748
- [13] Abbasi R. U. et al. [HiRes collaboration], 2008, *Phys. Rev. Lett.*, vol. 100 pp. 101101.
- [14] Abbasi, R. U., et al. [HiRes Collaboration], 2010, *Phys. Rev. Lett.*, 104, 161101
- [15] Abbasi R. U. et al. [HiRes collaboration], 2010, *ApJ*, 713, L64
- [16] Hopkins, A. M., & Beacom, J. F., 2006, *ApJ*, 651, 142.
- [17] Huchra, J. P., Macri, L. M., Masters, K. L., et al., 2012, *APJ Suppl.*, 199, 26
- [18] The JEM-EUSO Collaboration, 2012, arXiv:1204.5065
- [19] Rouilleé d'Orfeuil, B. et al., this conference, CR-TH-984
- [20] Tameda, Y., et al. [Telescope Array Collaboration] 2011, *Proc. of the 32nd ICRC, Beijing, China, Vol. 2, HE1.3*, 246
- [21] Abu-Zayyad, T. et al. [Telescope Array collaboration], 2012, *Phys. Rev. Lett.*, *submitted*, arXiv:1202.5141
- [22] Abu-Zayyad, T., et al. [Telescope Array Collaboration], 2012, arXiv:1205.5984
- [23] Wall, J. V., Jackson, C. A., Shaver, P. A., Hook, I. M., & Kellermann, K. I., 2005, *A&A*, 434, 133.
- [24] Zatsepin G. T. and Kuzmin V. A. 1966, *Sov. Phys. JETP Lett.* 4, 78